Birthdate for the Coronation paleocean: age of initial rifting in Wopmay orogen, Canada[1]

Paul F. Hoffman, Samuel A. Bowring, Robert Buchwaldt, and Robert S. Hildebrand

Abstract: The 1.9 Ga Coronation "geosyncline" to the west of Slave craton was among the first Precambrian continental margins to be identified, but its duration as a passive margin has long been uncertain. We report a new U–Pb (isotope dilution – thermal ionization mass spectrometry (ID–TIMS)) $^{207}Pb/^{206}Pb$ date of 2014.32 ± 0.89 Ma for zircons from a felsic pyroclastic rock at the top of the Vaillant basalt, which underlies the passive margin sequence (Epworth Group) at the allochthonous continental slope. A sandstone tongue within the basalt yields Paleoproterozoic (mostly synvolcanic) and Mesoarchean detrital zircon dates, of which the latter are compatible with derivation from the Slave craton. In contrast, detrital zircon grains from the Zephyr arkose in the accreted Hottah terrane have Paleoproterozoic and Neoarchean dates. The latter cluster tightly at 2576 Ma, indistinguishable from igneous zircon dates reported here from the Badlands granite, which is faulted against the Vaillant basalt and underlying Drill arkose. We interpret these data to indicate that Badlands granite belongs to the hanging wall of the collisional geosuture between Hottah terrane and the Slave margin, represented by the Drill–Vaillant rift assemblage. If 2014.32 ± 0.89 Ma dates the rift-to-drift transition and 1882.50 ± 0.95 Ma (revised from 1882 ± 4 Ma) the arrival of the passive margin at the trench bordering the Hottah terrane, the duration of the Coronation passive margin was ∼132 million years, close to the mean age of extinct Phanerozoic passive margins of ∼134 million years (see Bradley 2008).

Résumé : Le « géosynclinal » Coronation, 1,9 Ga, à l'ouest du craton des Esclaves a été parmi les premières bordures continentales précambriennes à être identifiées, mais le temps qu'il a servi de bordure passive demeure incertain depuis longtemps. Nous signalons une nouvelle datation U–Pb (ID–TIMS) $^{207}Pb/^{206}Pb$ de 2014,32 ± 0,89 Ma sur des zircons provenant d'une roche pyroclastique felsique au sommet du basalte Vaillant, lequel est sous la séquence de bordure passive (Groupe d'Epworth) à la pente continentale allochtone. Une langue de grès dans le basalte a donné, pour des zircons détritiques, des âges Paléoprotérozoïque (surtout synvolcanique) et Mésoarchéen; ce qui est, pour le Mésoarchéen, compatible avec une provenance du craton des Esclaves. Par contre, des grains de zircons détritiques provenant de l'arkose Zephyr dans le terrane accrété de Hottah ont donné des dates de Paléoprotérozoïque et de Néoarchéen. Ces dernières dates sont regroupées de manière serrée à 2576 Ma et ne peuvent être distinguées des dates de zircons ignés rapportées ici et provenant du granite Badlands, lequel est juxtaposé au basalte Vaillant et à l'arkose Drill par une faille. Selon nous, ces données indiquent que le granite Badlands appartient à l'éponte supérieure de la géosuture de collision entre le terrane de Hottah et la bordure des Esclaves, représentée par l'assemblage de distension Drill-Vaillant. Si 2014,32 ± 0,89 Ma constitue la date de la transition de distension à dérive et si 1882,50 ± 0,95 Ma (révisé de 1882 ± 4 Ma) représente l'arrivée de la bordure passive à la fosse en bordure du terrane de Hottah, alors la bordure passive Coronation aurait duré ~132 Ma, ce qui est près de l'âge moyen des bordures passives phanérozoïques disparues, soit ~134 Ma (voir Bradley 2008).

[Traduit par la Rédaction]

Introduction

The first pre-Mesozoic succession to be identified as a former continental terrace was the Neoproterozoic–Cambrian Adelaide "geosyncline" of South Australia (Sprigg 1952). In the then prevailing view that ocean basins were fixed and permanent, "the apparent disappearance of earlier [pre-Mesozoic] terraces forms a baffling problem of fundamental importance to geophysics and geology" (Kuenen 1950 p. 76). Sprigg suggested that "this problem is more apparent than real, and that many Beltian type miogeosynclines originated as continental terraces" (1952, p. 159).

Received 7 December 2009. Accepted 23 April 2010. Published on the NRC Research Press Web site at cjes.nrc.ca on 23 February 2011.

Paper handled by Associate Editor W. Davis.

P.F. Hoffman.[2,3] Department of Earth and Planetary Sciences, Harvard University, 20 Oxford St., Cambridge, MA 02138, USA; School of Earth and Ocean Sciences, University of Victoria, Box 1700, Victoria, BC V8W 2Y2, Canada.
S.A. Bowring and R. Buchwaldt. Department of Earth. Atmospheric, and Planetary Sciences, Massachusetts Institute of Technology, Cambridge, MA 02139, USA.
R.S. Hildebrand. 1401 N. Camino de Juan, Tucson, AZ 85745, USA.

[1]This article is one of a series of papers published in this Special Issue on the theme of *Geochronology* in honour of Tom Krogh.

[2]Corresponding author (e-mail: paulfhoffman@yahoo.com).
[3]Present address: 1216 Montrose Ave., Victoria, BC, V8T 2K4, Canada.

Fig. 1. Tectonic elements of Wopmay orogen and Slave craton, showing locations of the Vaillant basalt-dominated rift assemblage (Melville Group), Lac de Gras dyke swarm (Buchan et al. 2009), and related Booth River intrusive suite (BRIS). Wopmay orogen includes the Great Bear magmatic arc (1.88–1.84 Ga), the Hottah arc terrane that was accreted to the Coronation margin at 1.88 Ga, and the Asiak foreland thrust-fold belt (shown expanded on the left) comprised of rift, passive margin, and foredeep deposits deformed by the Hottah–Slave collision (Calderian orogeny). TK is the Turmoil klippe of Hottah terrane (Hildebrand et al. 2010*a*). The Taltson–Thelon magmatic arc formed on the active margin of the Archean Rae craton prior to and during its collision with the Archean Slave craton at 1.97 Ga. The Lac de Gras dyke swarm is one of many distinct Paleoproterozoic dyke swarms in the Slave craton.

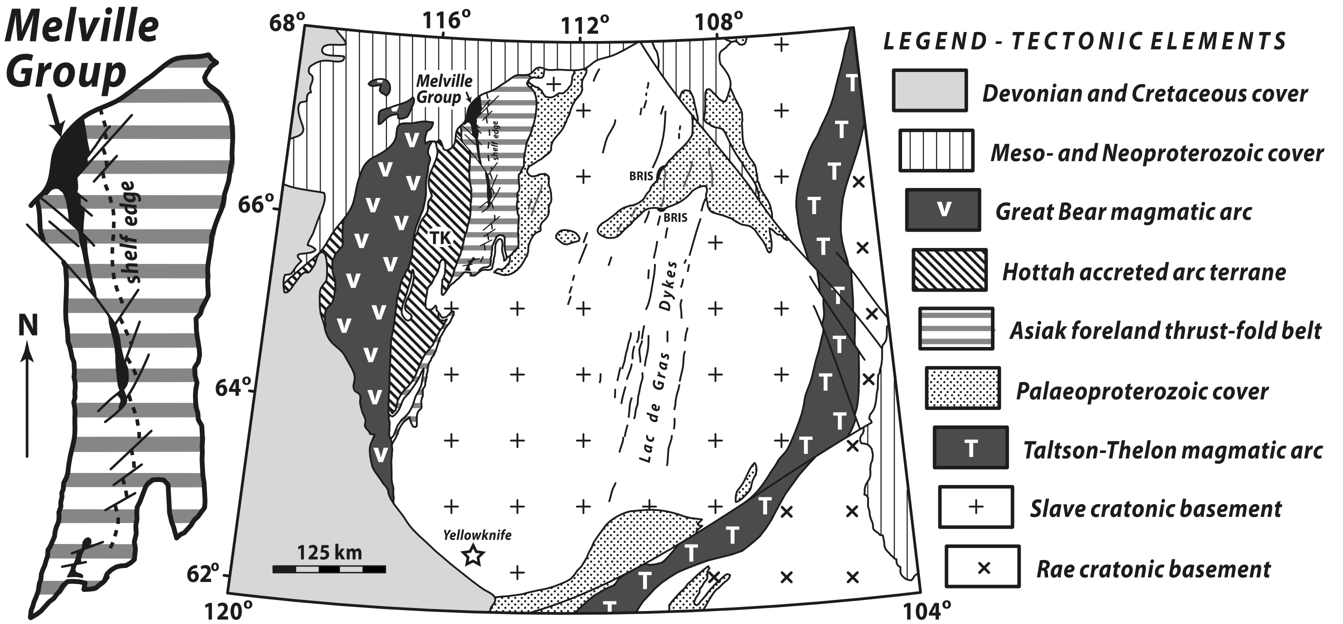

After the plate tectonics revolution of 1962–67, the search for very old continental terraces took on new impetus: when did plate tectonics begin? The first well-documented continental terrace of deep Precambrian age was the late Paleoproterozoic (ca. 1.9 Ga) Coronation "geosyncline" in the northwest of the Canadian Shield (Fraser et al. 1971; Hoffman 1973, 1980; Grotzinger 1986). It was compared with the Appalachian "geosynclinal" succession (Hoffman et al. 1970) in an early attempt to estimate its longevity in the absence of direct and reliable geochronological constraints.

As now understood, the Appalachian passive margin lasted ∼75 million years, from continental breakup ca. 540 Ma (Cawood et al. 2001) until its (diachronous) collision with the Taconic intra-oceanic island arc ca. 465 Ma (Bradley 2008). In the northern Appalachians, an active margin existed thereafter for an additional ∼40 million years until terminal Laurentia–Baltica collision in the late Silurian (van Staal et al. 1998, 2009). In the central and southern Appalachians, an active margin persisted for ∼145 million years, until terminal Laurrussia–Gondwana collision ca. 310–320 Ma (Nance and Linnemann 2008).

Wopmay orogen (Figs. 1 and 2) is the former mountain belt resulting from the closure of the Coronation 'paleocean.' The passive margin stage terminated with collision between the Hottah terrane, a continental magmatic arc, and the west-facing rifted margin of Slave craton (Hildebrand et al. 2010*a*). The age of the Hottah–Slave collision is constrained by a volcanic tuff dated at 1882 ± 4 Ma from near the base of the syn-collisional foredeep succession (Hoffman 1987*b*; Bowring and Grotzinger 1992). Following the arc–continent collision, the west-facing Great Bear magmatic arc was active between 1.88 and 1.84 Ga, indicating eastward dipping subduction at that time (Hoffman and McGlynn 1977; Bowring 1985; Hoffman and Bowring 1984; Hildebrand et al. 1987, 2010*b*; Hoffman 1987*a*; Cook et al. 1999). The Great Bear magmatic zone bisected the Hottah terrane, isolating to the east a synformal allochthon named the Turmoil klippe (Fig. 1; Hildebrand et al. 2010*a*). Terminal collision is recorded throughout the orogen by a system of conjugate transcurrent faults that postdate the youngest Great Bear plutons (ca. 1.84 Ga) and predate the mafic Cleaver dykes dated at 1740 $^{+5}_{-4}$ Ma (Irving et al. 2004). Accordingly, the active stage of the Coronation margin began at 1.88 Ga and ended between 1.84 and 1.74 Ga, a duration directly comparable to the Appalachians (i.e., 40–140 million years).

The age of continental breakup and initiation of the Coronation passive margin, however, has long been uncertain. Bimodal volcanism and coarse clastic sedimentation (Akaitcho Group) in the internal Wopmay orogen ca. 1.90–1.89 Ga (Easton 1981, 1983; Bowring 1985; Hoffman and Bowring 1984) were originally taken as related to initial rifting of the cratonic margin. This assumption limited the duration of the passive margin to less than 10 million years (Hoffman and Bowring 1984). Subsequent Nd and Pb isotopic studies (Villeneuve 1988; Bowring and Podosek 1989; Housh et al. 1989), reinforced by new mapping (Hildebrand et al. 1990, 1991, 2010*b*), made it clear that the Akaitcho Group represents rifting of the Hottah magmatic arc and its latest Neoarchean (geon 25) basement. It does not represent rifting of the autochthonous Slave craton, which is composed of older, albeit dominantly Neoarchean rocks. This

Fig. 2. Sample locations (numbered circles) in northern Wopmay orogen for dates reported in this paper: (1) Felsic tuff at top of Vaillant basalt (Melville Group); (2) Tongue of Drill arkose within Vaillant basalt; (3) Badlands granite; (4) Zephyr arkose (Akaitcho Group) in Turmoil klippe of Hottah terrane; (5) Fontano tuff (Recluse Group) of Calderian foredeep. Map modified from Hildebrand et al. (2010*a*).

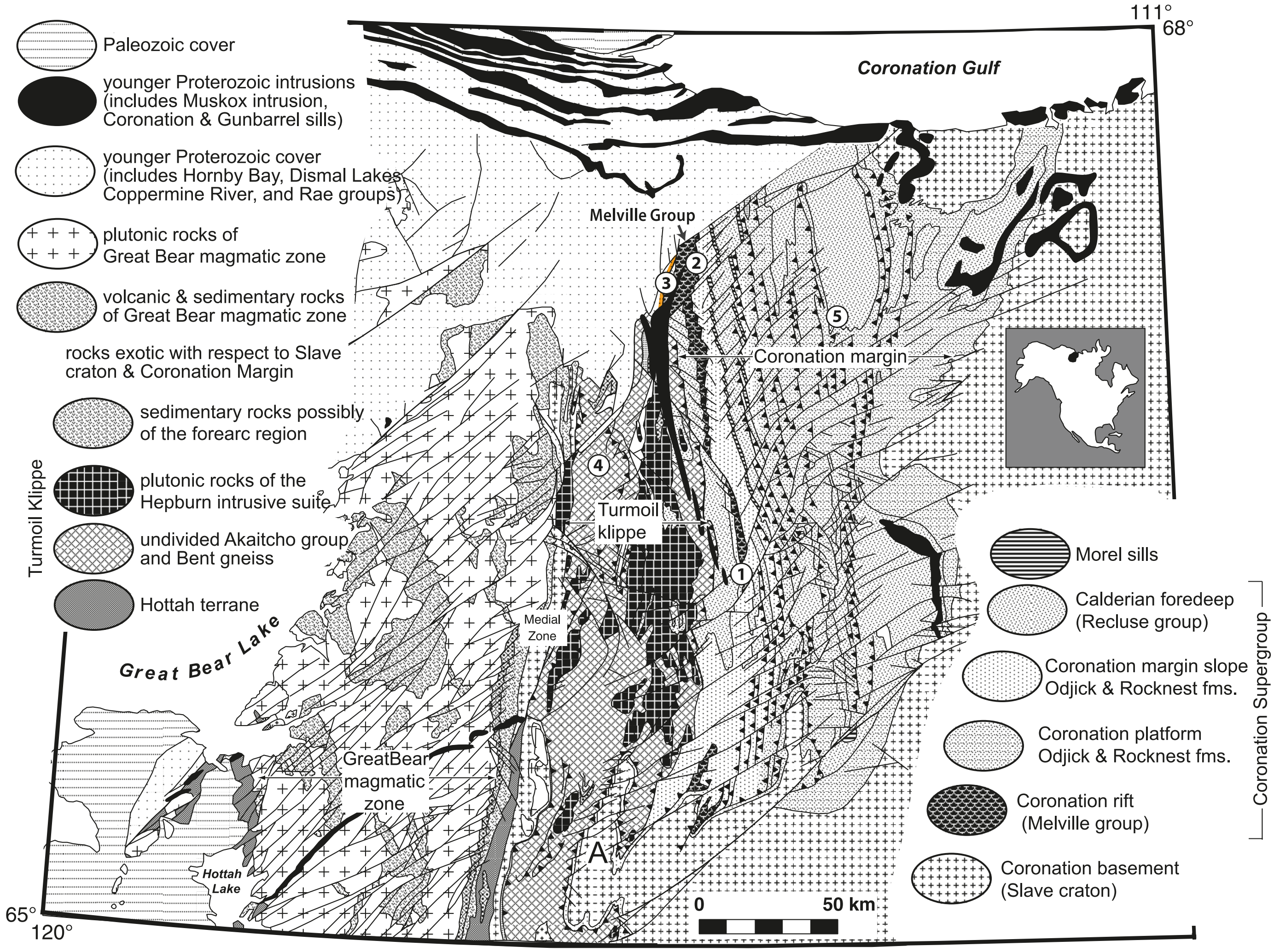

finding was confirmed by U–Pb zircon dating of tuffs as old as 1969 ± 1 Ma in sequence stratigraphic correlatives of the Coronation passive margin in the Kilohigok basin on the eastern margin of the Slave craton (Bowring and Grotzinger 1992). Thus, geochronological data consort with isotopic tracers and field mapping to indicate that initial rifting of the passive margin must be older than ca. 1.97 Ga.

The U–Pb geochronology that aided the development of tectonic models for Wopmay orogen was largely completed in the early 1980s, using a traditional multigrain approach, some of the grains being air abraded (Krogh 1982) zircons. This paper represents our continued interest in applying the methods of high-precision geochronology to elucidate tectonic processes in the Paleoproterozoic. Our approach has been greatly influenced by Tom Krogh, who recognized and demonstrated that high-precision dating was not only possible in very ancient rocks, if discordance could be eliminated, but would allow tectonic models to be tested in detail (Krogh and Davis 1971). The new ID–TIMS data for single grains reported here reflect much improved analytical procedures, including much lower analytical blanks and the use of chemical abrasion (CA) or chemical abrasion – thermal ionization mass spectrometry (CA–TIMS) (Mattinson 2005). The new dates include (1) igneous zircons from a felsic tuff at the top of a rift-related mafic sequence (Vaillant basalt of Hoffman and Pelletier 1982) situated stratigraphically beneath the passive margin sequence (Epworth Group) at the cratonic margin; (2) detrital zircons from a clastic sedimentary tongue (Drill arkose of Hoffman and Pelletier 1982) within the Vaillant basalt; (3) igneous zircons from an Archean granite that is in fault contact with the Vaillant basalt and Drill arkose; (4) detrital zircons from the Zephyr arkose (Akaitcho Group) in the Turmoil klippe of Hottah terrane; and (5) igneous zircons from the previously dated volcanic ash bed in the basal foredeep strata (Fontano shale), deposited above the passive margin during its descent into the trench bordering the Hottah terrane. We infer that the age of the felsic tuff in the Vaillant

Fig. 3. (*a*) Tectonic map of the Melville Group (Cloos nappe), showing its relation to slope-facies allochthon of Epworth Group (Esl), syncline of foredeep deposits (dotted) straddling the outer edge of the Rocknest carbonate platform (Esh), and Marceau thrust sheet (Hoffman et al. 1980), carrying the Turmoil klippe of Hottah terrane (Hildebrand et al. 2010*a*), Hepburn intrusive suite and possible rise-facies equivalents of Epworth Group (Eri). (*b*) Geological map of northern end of Cloos nappe, showing stratigraphic and structural relations within Melville Group, and Badlands granite contact (modified after Hoffman and Pelletier 1982). Open stars indicate geochronology sample sites (see Fig. 5*f* for location map of Vaillant tuff sample SAB91–73).

basalt closely approximates the age of the rift-to-drift transition at the (present) western margin of the craton, providing a birthdate for the Coronation passive margin and paleocean.

Initial-rift assemblage

In Wopmay orogen (Figs. 1–3), subaqueous basalt and associated sedimentary rocks of the Melville Group (Hoffman and Hall 1993) are exposed stratigraphically beneath the passive margin sedimentary sequence (Epworth Group) in an allochthonous anticlinorium dubbed "Cloos nappe" (Hoffman and Pelletier 1982). Cloos nappe rides on the back of the easternmost allochthon carrying slope facies of the Epworth Group (Fig. 3). Its leading edge lies 5–10 west of the allochthonous shelf edge of the Rocknest Formation (Fig. 4), the passive margin carbonate platform (Grotzinger 1986; Hoffman and Tirrul 1994). Cloos nappe is tectonically analogous to the Long Range – Green Mountain – South Mountain – Blue Ridge anticlinorium of the Appalachians (Hibbard et al. 2005). The Melville Group consists in ascending order of the Drill arkose, Vaillant basalt and Stanbridge dolomite (Hoffman and Pelletier 1982). These formations were originally assigned to the Akaitcho Group (Hoffman and Pelletier 1982) but, as discussed below, this correlation is demonstrably incorrect. The Badlands granite (Hoffman and Pelletier 1982) discordantly truncates the Melville Group in the extreme northwest of Cloos nappe, just before it disappears beneath Mesoproterozoic cover (Dismal Lakes Group) of the Coppermine homocline (Fig. 3).

Drill arkose

A sequence of medium- to thick-bedded, feldspathic and subfeldspathic granulestone turbidites is exposed in the core of the anticlinorium adjacent to the Badlands granite (Fig. 3*b*). The turbidites are intercalated with black carbonaceous pelite and semipelite, and beds of quartz- and locally granite-pebble conglomerate, commonly with outsize blocks of dolomite up to 3 m in diameter. Mafic tuffs, flows and sills occur sporadically within the sedimentary rocks. Small felsic flows and crystal-rich rhyolite tuffs, associated with beds of carbonate or jasper, occur locally. The base of the arkose is not exposed, but a distinctive plagioclase-phyric flow at the base of the Vaillant basalt makes the top of the arkose easy to map around the south-plunging, synformally refolded crest of the anticlinorium (Hoffman and Pelletier 1982).

Vaillant basalt

A thick pile of mafic pillow lava and hyaloclastite breccia forms the main part of the anticlinorial succession (Hoffman et al. 1978; Hoffman and Pelletier 1982). Tongues of feldspathic sandstone (Drill arkose) occur between basalt ridges in the northernmost exposures of Cloos nappe (Fig. 3*b*), but the degree to which they lie stratigraphically within or beneath the Vaillant basalt is unclear. Silicified flow-tops occur throughout the sequence and felsic tuffs much more sparingly. At the top of the volcanic pile, mafic flows are interstratified with the Stanbridge dolomite (Fig. 3*b*).

At Vaillant Lake (Fig. 5*f*), the anticlinorium plunges southward beneath the Odjick Formation, the lower clastic part of the Coronation passive margin sequence (Fig. 4). On the peninsula at the north end of the lake, the basalts are conformably overlain by a felsic tuff. Above the tuff is the Stanbridge dolomite, which, in turn, is overlain by the Odjick Formation in a slope facies (i.e., semipelite with quartzite turbidite, contourite, and channelized debrite). The tuff was discovered in 1991 during field work dedicated to geochronology.

Stanbridge dolomite

At least 850 m of cherty stromatolitic dolomite and cross-bedded quartz-arenaceous dolomite overlie the Vaillant basalt in the southern third of the anticlinorium (Hoffman et al. 1978; Hoffman and Pelletier 1982). A major facies change takes place in the central segment of the anticlinorium between 66°40′N and 67°00′N latitude (Fig. 3). Shallow-water stromatolitic dolomite to the south passes into spectacular sedimentary breccias, composed of angular blocks of shallow-water dolomite up to 20 m in size, that intertongue northward with thin-bedded rhythmic dololutite and black carbonaceous pelite, locally tuffaceous. The facies change takes place over a strike length of 40 km and is interpreted as a highly oblique section of a platform-slope-basin facies change. In the transition zone, the northern basinal facies appears at the base of the sequence and shallow-water facies at the top, indicating basinward progradation of the platform. There is no comparable north–south facies change in the Vaillant or Odjick formations.

Between 66°37′N and 67°00′N latitude, the Stanbridge dolomite is inferred to be overlain depositionally by quartzose semipelite of the Odjick Formation on the east limb of the anticline (Fig. 3*a*), although the contact is generally covered. To the north, the dolomite thins and disappears (Fig. 3*b*). This is attributed in part to the facies change within the Stanbridge dolomite and in part to a fault that thrusts Vaillant basalt eastward over Odjick semipelite at the level of exposure. On the west limb of the anticline, the Stanbridge dolomite is overlain by the Odjick Formation in the southern half of the structure, but to the north it is faulted against black carbonaceous slate (Fontano Formation) of the overlying foredeep sequence (Fig. 3*a*). The fault is inferred to be a west-side-down normal fault that was active during foredeep subsidence, based on the occurrence of isolated blocks of Stanbridge dolomite within the Fontano slate up to 1 km west of the Stanbridge–Fontano contact

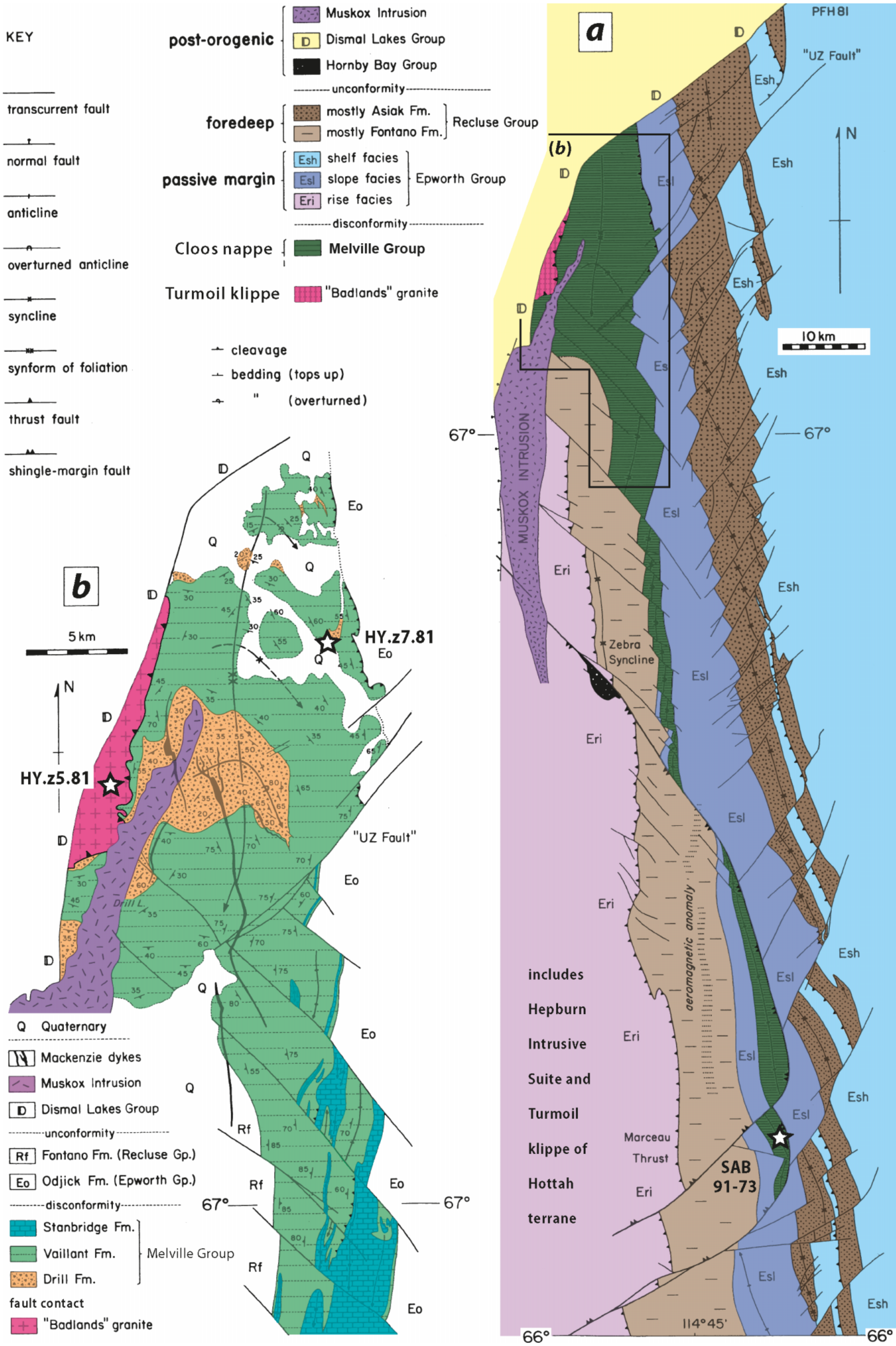
KEY
transcurrent fault
normal fault
anticline
overturned anticline
syncline
synform of foliation
thrust fault
shingle-margin fault
post-orogenic
Muskox Intrusion
Dismal Lakes Group
Hornby Bay Group
unconformity
foredeep
mostly Asiak Fm.
mostly Fontano Fm.
Recluse Group
passive margin
Esh shelf facies
Esl slope facies
Eri rise facies
Epworth Group
disconformity
Cloos nappe
Melville Group
Turmoil klippe
"Badlands" granite
cleavage
bedding (tops up)
" (overturned)
a
(b)
PFH 81
"UZ Fault"
N
10 km
67°
66°
MUSKOX INTRUSION
Zebra Syncline
aeromagnetic anomaly
includes Hepburn Intrusive Suite and Turmoil klippe of Hottah terrane
Marceau Thrust
SAB 91-73
114°45'
b
5 km
HY.z7.81
HY.z5.81
Drill L.
Q Quaternary
Mackenzie dykes
Muskox Intrusion
Dismal Lakes Group
unconformity
Rf Fontano Fm. (Recluse Gp.)
Eo Odjick Fm. (Epworth Gp.)
disconformity
Stanbridge Fm.
Vaillant Fm.
Drill Fm.
Melville Group
fault contact
"Badlands" granite

Fig. 4. Palinspastic restoration of the Coronation continental terrace (datum top of Rocknest carbonate platform) and subsequent foredeep deposits, showing new and published U–Pb age constraints (Bowring and Grotzinger 1992; Davis and Bleeker 2007). Initial rifting terminated soon after 2014 Ma and the subsequent passive margin stage ended in 1882 Ma when the Rocknest carbonate platform foundered into the Calderian foredeep. Tectonic shortening associated with Calderian collision between the east-facing Hottah arc and the Slave margin caused the initial rift basin (Melville Group) to be structurally inverted as Cloos nappe.

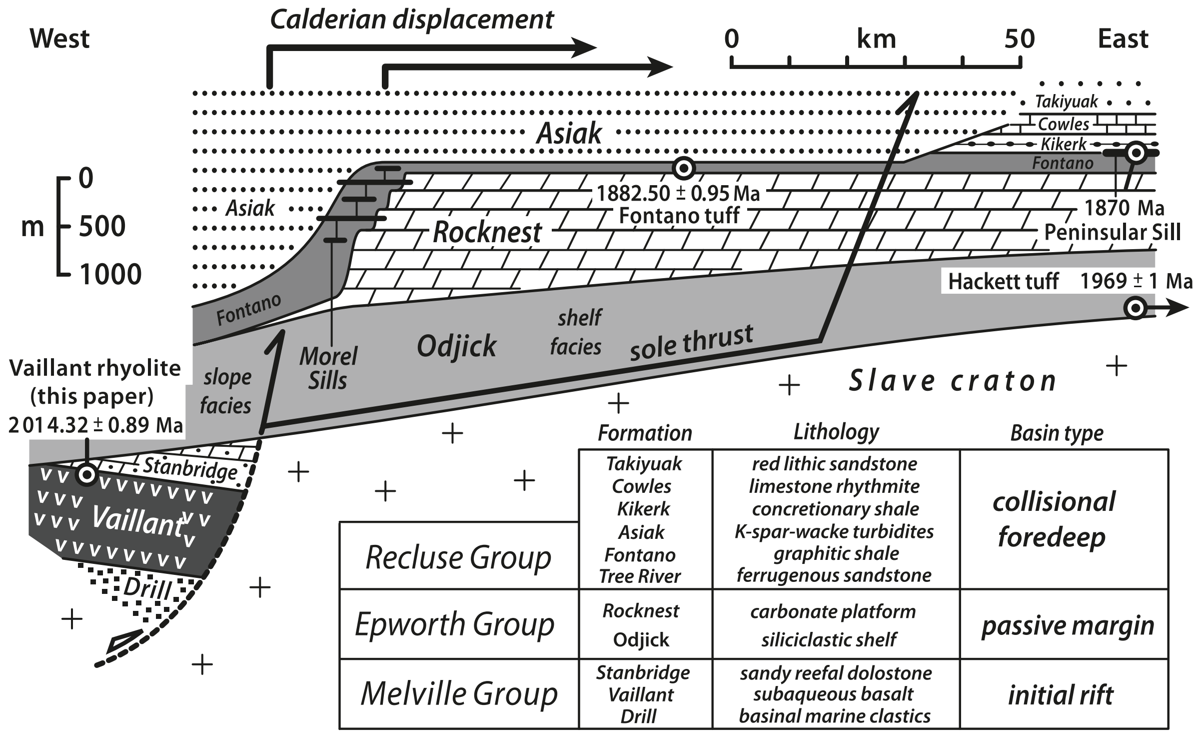

(Hoffman et al. 1978). The throw of the fault is uncertain and the Stanbridge–Fontano juxtaposition might alternatively reflect sedimentary bypass, or even submarine erosion, during passive margin sedimentation on the continental slope (Hoffman and Pelletier 1982).

Badlands granite

An epizonal leucocratic monzogranite with chloritized amphibole, accessory tourmaline and abundant pegmatite truncates the core of the anticlinorium for 14 km between the northern prong of the Muskox ultramafic intrusion (1.27 Ga) and the Coppermine homocline (Hoffman and Pelletier 1982; Hoffman and Tirrul 1994; Hildebrand 2011). The granite is weakly foliated and altered by paleoweathering beneath the Mesoproterozoic unconformity and contact metamorphism associated with the Muskox intrusion. The irregular contact of the granite is sharp and discordant with respect to the Drill arkose and Vaillant basalt (Fig. 3*b*), and was originally interpreted as intrusive despite the absence of a metamorphic aureole or granite dykes in the arkose or basalt (Hoffman and Pelletier 1982).

U–Pb ID–TIMS geochronology

Zircons from Paleoproterozoic rocks often have complex and protracted histories that result in open-system behavior, most often Pb-loss, which can compromise the accuracy and decrease the precision of calculated dates. The dual decay of ^{238}U and ^{235}U to ^{206}Pb and ^{207}Pb, respectively, permits an internal test of open-system behavior, thereby allowing one to validate the accuracy of the calculated dates. If it can be established that a zircon behaved as a closed system (i.e., it is concordant), then the ^{207}Pb/^{206}Pb date is permissible, the absolute uncertainty of which decreases with the age of the mineral for a constant analytical error. It is, therefore, the most precise approach for dating Paleoproterozoic and older rocks (e.g., Mattinson 1987). In concordant minerals with high ratios of radiogenic to initial Pb (Pb* to Pb_c), the ^{207}Pb/^{206}Pb date is the most *accurate* date as well. As Tom Krogh demonstrated more than 25 years ago, pretreating zircons can often minimize or eliminate domains within the crystals that have experienced open-system behavior. A recent advance in zircon pretreatment techniques, the chemical abrasion technique or CA–TIMS (Mattinson 2005), has greatly improved our ability to isolate closed-system domains of zircon. This, in conjunction with improved laboratory blanks, has enabled the generation of weighted mean ^{207}Pb/^{206}Pb dates with uncertainties of ca. 1 Ma or less. This, in turn, allows for testing of tectonic models of the development of orogenic belts. The CA–TIMS zircon analyses form coherent clusters for which most of the scatter can be explained by analytical uncertainties alone. Most high-precision data from CA–TIMS-treated zircon exhibit a slight but systematic age discordance (manifested by older ^{207}Pb/^{206}Pb dates relative to the corresponding Pb/U dates) likely because of inaccuracy in one or both of the U decay con-

Table 1. Isotopic data along with details of fractionation and blank corrections.

	Composition				Isotopic ratios							Dates (Ma)						
	Th/U[a]	Pb*[b] (pg)	Pbc[c] (pg)	Pb*/Pbc[d]	$^{206}Pb^{e}/^{204}Pb$	$^{206}Pb^{f}/^{238}U$	±2σ (%)	$^{207}Pb^{f}/^{235}U$	±2σ (%)	$^{207}Pb^{f}/^{206}Pb$	±2σ (%)	$^{206}Pb^{g}/^{238}U$	±2σ (abs.)	$^{207}Pb^{g}/^{235}U$	±2σ (abs)	$^{207}Pb^{g}/^{206}Pb$	±2σ (abs.)	Corr. Coef.
Vaillant tuff (SB91–73): Zircon — GPS: 66°14′N, 114°31.1′W																		
Chemical abrasion																		
z7	0.63	35.5	1.59	22	1254	0.36548	0.240	6.244	0.50	0.123920	0.310	2008.1	4.1	2010.7	4.4	2013.4	5.5	0.89
z8	0.57	46.6	1.08	43	2435	0.36629	0.240	6.262	0.28	0.123980	0.086	2011.9	4.1	2013.1	2.5	2014.3	1.5	0.96
z9	0.67	37.5	1.08	35	1927	0.36631	0.210	6.266	0.33	0.124050	0.210	2012.0	3.6	2013.7	2.9	2015.3	3.8	0.78
z10	0.59	39.4	0.81	49	2741	0.36748	0.190	6.284	0.25	0.124020	0.110	2017.5	3.3	2016.2	2.2	2014.8	2.0	0.90
z11	0.85	48.6	0.99	49	2605	0.36697	0.097	6.274	0.19	0.124000	0.140	2015.1	1.7	2014.9	1.7	2014.6	2.4	0.72
z12	0.56	58.9	0.43	137	7727	0.36669	0.100	6.266	0.16	0.123930	0.100	2013.8	1.8	2013.7	1.4	2013.6	1.8	0.79
z13	0.71	131.0	0.40	329	17919	0.36724	0.120	6.288	0.15	0.124178	0.065	2016.4	2.1	2016.7	1.3	2017.1	1.2	0.89
Legacy data (Air abrasion)																		
Z1	0.63	292.2	5.47	53	2942	0.36108	0.263	6.169	0.29	0.123909	0.105	1987.3	5.2	2000.1	5.7	2013.3	2.1	0.93
Z2	0.57	2098.9	10.12	207	11104	0.35689	0.090	6.100	0.11	0.123962	0.070	1967.4	1.8	1990.2	2.3	2014.0	1.4	0.79
Z3	0.61	1810.5	10.43	174	9185	0.35396	0.080	6.050	0.09	0.123958	0.042	1953.5	1.6	1983.0	1.8	2014.0	0.8	0.89
Z4	0.54	444.6	5.98	74	4122	0.34879	0.193	5.964	0.21	0.124008	0.088	1928.8	3.7	1970.6	4.2	2014.7	1.8	0.91
Z5	0.59	973.5	8.96	109	5809	0.34783	0.168	5.949	0.17	0.124053	0.046	1924.2	3.2	1968.5	3.4	2015.3	0.9	0.96
Z6	0.59	973.3	8.76	111	5947	0.34771	0.168	5.948	0.18	0.124069	0.051	1923.6	3.2	1968.3	3.5	2015.6	1.0	0.96
Z8	0.72	192.2	12.39	16	804	0.33491	0.373	5.728	0.39	0.124053	0.090	1862.1	6.9	1935.7	7.5	2015.3	1.8	0.97
Z9	0.82	156.9	2.76	57	3126	0.36558	0.359	6.249	0.36	0.123981	0.059	2008.6	7.2	2011.4	7.3	2014.3	1.2	0.99
Badlands granite (HY.z5.81): Zircon — GPS: 67°11′N, 115°10.0′W																		
Chemical abrasion																		
z1	0.76	376.0	0.89	424	22128	0.48882	0.069	11.583	0.11	0.171866	0.044	2565.6	1.5	2571.3	1.0	2575.9	0.8	0.94
z3	0.70	362.0	1.18	308	16307	0.48998	0.099	11.618	0.13	0.171977	0.055	2570.6	2.1	2574.2	1.2	2577.0	0.9	0.92
z4	0.83	85.7	2.65	32	1682	0.49214	0.170	11.666	0.22	0.171930	0.120	2579.9	3.7	2578.0	2.1	2576.5	2.0	0.86
z5	0.82	59.3	0.73	81	4185	0.49227	0.140	11.662	0.16	0.171820	0.071	2580.5	2.9	2577.7	1.5	2575.5	1.2	0.89
z6	0.81	530.0	0.86	618	31969	0.49073	0.080	11.630	0.10	0.171882	0.026	2573.9	1.7	2575.1	1.0	2576.1	0.5	0.98
z7	0.87	283.0	0.30	937	47912	0.49055	0.076	11.619	0.11	0.171789	0.050	2573.1	1.6	2574.2	1.0	2575.2	0.9	0.91
z8	0.76	140.0	1.65	85	4442	0.48930	0.270	11.594	0.28	0.171880	0.086	2567.4	5.6	2572.2	2.7	2576.0	1.5	0.95
z9	0.59	148.0	0.52	285	15453	0.49116	0.130	11.636	0.16	0.171830	0.078	2575.7	2.7	2575.6	1.5	2575.6	1.3	0.88
z11	0.64	467.0	0.56	827	44266	0.49036	0.094	11.619	0.12	0.171849	0.048	2572.2	2.0	2574.2	1.1	2575.7	0.8	0.92
Zephyr arkose (VS80–13): Zircon — GPS: 66°32.2 N, 115°40.4′W																		
Chemical abrasion																		
z17	0.81	212.0	0.95	224	11575	0.49107	0.083	11.633	0.13	0.171810	0.077	2575.3	1.8	2575.4	1.2	2575.4	1.3	0.82
z18	0.75	82.1	1.18	70	3672	0.49129	0.130	11.642	0.17	0.171870	0.078	2576.2	2.8	2576.1	1.6	2575.9	1.3	0.89
z19	0.65	132.0	1.24	106	5694	0.48994	0.150	11.605	0.19	0.171790	0.083	2570.4	3.3	2573.1	1.7	2575.1	1.4	0.90
z20	0.96	153.0	2.13	72	3624	0.49045	0.060	11.623	0.12	0.171880	0.079	2572.6	1.3	2574.5	1.1	2576.0	1.3	0.77
z21	0.84	185.0	1.62	115	5912	0.49030	0.078	11.624	0.12	0.171950	0.062	2572.0	1.6	2574.6	1.1	2576.7	1.1	0.89
z23	0.61	66.2	0.69	96	5169	0.49108	0.077	11.632	0.13	0.171790	0.079	2575.3	1.6	2575.2	1.2	2575.1	1.3	0.81
z25	0.64	140.0	1.06	132	7097	0.49004	0.100	11.611	0.13	0.171844	0.056	2570.8	2.2	2573.6	1.2	2575.7	1.0	0.91
z26	0.59	105.0	2.69	39	2132	0.49063	0.089	11.622	0.17	0.171800	0.150	2573.4	1.9	2574.5	1.5	2575.3	2.5	0.44
z27	0.87	159.0	2.07	77	3930	0.49063	0.065	11.634	0.11	0.171980	0.062	2573.4	1.4	2575.4	1.0	2577.0	1.1	0.86
z29	0.91	90.3	0.73	123	6266	0.49089	0.099	11.628	0.13	0.171800	0.061	2574.5	2.1	2575.0	1.3	2575.3	1.1	0.90
z31	0.45	16.4	0.63	26	1542	0.33980	0.610	5.438	0.71	0.116070	0.390	1886.0	10.0	1890.8	6.1	1896.5	7.0	0.84
z33	0.54	38.8	0.41	94	5362	0.34155	0.055	5.456	0.12	0.115860	0.096	1894.1	0.9	1893.7	1.1	1893.3	1.7	0.64
z34	0.50	35.1	1.42	25	1440	0.33902	0.190	5.431	0.39	0.116190	0.300	1882.0	3.1	1889.8	3.3	1898.4	5.4	0.66
z35	0.91	94.4	0.62	152	7954	0.33698	0.074	5.389	0.13	0.115974	0.060	1872.1	1.2	1883.0	1.1	1895.1	1.1	0.95
Legacy data (Air abrasion)																		

Published by NRC Research Press

Table 1 (*concluded*).

	Composition				Isotopic ratios							Dates (Ma)						
	Th/U[a]	Pb*[b] (pg)	Pbc[c] (pg)	Pb*/Pbc[d]	$^{206}Pb/^{204}Pb$[e]	$^{206}Pb/^{238}U$[f]	±2σ (%)	$^{207}Pb/^{235}U$[f]	±2σ (%)	$^{207}Pb/^{206}Pb$[f]	±2σ (%)	$^{206}Pb/^{238}U$[g]	±2σ (abs.)	$^{207}Pb/^{235}U$[g]	±2σ (abs)	$^{207}Pb/^{206}Pb$[g]	±2σ (abs.)	Corr. Coef.
Z4	11.36	454.4	4.06	112	1719	0.36069	0.125	6.225	0.19	0.125179	0.139	1985.4	2.5	2008.0	3.9	2031.3	2.8	0.70
Z5	0.54	251.4	5.68	44	2372	0.33096	0.195	5.283	0.23	0.115779	0.115	1843.0	3.6	1866.2	4.3	1892.0	2.2	0.86
Z6	1.20	109.1	4.01	27	1278	0.36655	0.164	6.365	0.23	0.125930	0.161	2013.2	3.3	2027.4	4.8	2041.9	3.3	0.73
Z7	0.33	664.1	6.89	96	5372	0.30913	0.115	4.872	0.13	0.114305	0.060	1736.4	2.0	1797.4	2.3	1869.0	1.1	0.89
Z8	0.32	447.1	3.83	117	6137	0.32230	0.097	7.705	0.11	0.173382	0.056	1800.9	1.7	2197.2	2.5	2590.6	1.4	0.87
Z9	0.50	169.8	3.99	43	2305	0.30886	0.151	4.907	0.20	0.115223	0.132	1735.1	2.6	1803.4	3.7	1883.4	2.5	0.76
Z10	0.28	225.8	4.54	50	2834	0.33507	0.116	5.563	0.14	0.120404	0.084	1862.9	2.2	1910.3	2.8	1962.2	1.6	0.82
Z11	0.72	448.6	48.86	9	475	0.33782	0.108	5.410	0.18	0.116139	0.134	1876.2	2.0	1886.4	3.4	1897.6	2.5	0.67
Z12	0.43	561.4	7.32	77	4024	0.36393	0.108	6.995	0.13	0.139412	0.076	2000.8	2.2	2110.9	2.8	2219.9	1.7	0.82
Z13	0.24	226.2	10.27	22	1169	0.40873	0.167	9.374	0.20	0.166344	0.112	2209.1	3.7	2375.3	4.8	2521.2	2.8	0.84
Z14	0.15	242.3	8.11	30	1753	0.28578	0.121	4.529	0.15	0.114946	0.079	1620.4	2.0	1736.4	2.5	1879.0	1.5	0.84
Z15	0.19	210.8	8.63	24	1384	0.20899	0.151	3.296	0.20	0.114369	0.133	1223.5	1.8	1480.0	3.0	1870.0	2.5	0.76
Z16	0.28	128.3	7.02	18	1033	0.25408	0.119	4.052	0.22	0.115658	0.181	1459.5	1.7	1644.7	3.7	1890.2	3.4	0.60
Fontano tuff (Ash bed A): Zircon — GPS: 67 03.3′N, 113 45.0’W																		
Chemical abrasion																		
z2	0.47	54.7	0.57	96	5590	0.33773	0.089	5.363	0.14	0.115175	0.086	1875.7	1.5	1879.0	1.2	1882.6	1.6	0.80
z3	0.51	22.0	0.65	34	1960	0.33927	0.250	5.378	0.33	0.114970	0.180	1883.2	4.1	1881.4	2.8	1879.5	3.3	0.84
z4	0.58	71.9	0.57	127	7174	0.33828	0.110	5.372	0.16	0.115180	0.092	1878.4	1.9	1880.4	1.4	1882.7	1.7	0.82
z5	0.49	47.8	0.93	51	2957	0.33881	0.170	5.381	0.23	0.115190	0.140	1881.0	2.8	1881.8	2.0	1882.8	2.5	0.81
z6	0.52	28.3	1.27	22	1293	0.33865	0.170	5.384	0.30	0.115310	0.220	1880.2	2.8	1882.3	2.6	1884.7	3.9	0.71
z7	0.48	11.6	0.75	16	915	0.33840	0.290	5.371	0.43	0.115120	0.330	1879.0	4.7	1880.3	3.7	1881.7	6.0	0.64
Drill arcose (HY.z7): Zircon — GPS: 67°15′N, 114°55.0′W																		
Chemical abrasion																		
z2	1.27	56.9	0.45	128	6200	0.36661	0.250	6.273	0.27	0.124110	0.090	2013.4	4.3	2014.8	2.4	2016.1	1.6	0.94
z3	1.36	110.0	1.34	82	3939	0.36667	0.160	6.278	0.21	0.124180	0.120	2013.7	2.7	2015.4	1.9	2017.2	2.2	0.82
z4	1.27	95.0	1.87	51	2472	0.36710	0.290	6.279	0.33	0.124060	0.130	2015.6	5.1	2015.6	2.9	2015.5	2.2	0.92
z5	1.39	33.2	0.78	42	2029	0.36670	0.630	6.278	0.66	0.124160	0.170	2014.0	11.0	2015.4	5.8	2016.9	3.0	0.97
z8	1.41	59.9	0.43	139	6560	0.36623	0.210	6.269	0.25	0.124150	0.120	2011.6	3.7	2014.2	2.2	2016.8	2.1	0.88
z10	1.36	81.6	0.61	134	6400	0.36750	0.280	6.290	0.30	0.124139	0.076	2017.4	4.9	2017.0	2.6	2016.5	1.4	0.97
z11	1.49	44.6	0.49	92	4294	0.36520	0.360	6.244	0.39	0.124020	0.130	2006.7	6.2	2010.7	3.4	2014.8	2.3	0.95
z13	1.30	34.5	0.75	46	2236	0.36758	0.220	6.301	0.28	0.124330	0.150	2018.0	3.9	2018.6	2.5	2019.3	2.7	0.84
Air abrasion																		
z14	0.47	550.0	4.05	136	6986	0.66202	0.075	25.695	0.11	0.281500	0.049	3275.0	1.9	3335.0	1.1	3371.3	0.8	0.91
z18	1.20	68.8	4.03	17	857	0.36540	0.540	6.246	0.63	0.123990	0.290	2007.7	9.2	2011.0	5.5	2014.3	5.1	0.89
z19	1.01	86.4	0.43	201	10060	0.41974	0.130	8.955	0.16	0.154740	0.076	2259.3	2.5	2333.5	1.4	2399.0	1.3	0.87
z20	1.11	22.6	5.54	11	619	0.41840	0.534	8.587	1.15	0.148840	0.887	2253.2	10.1	2295.1	10.5	2332.6	15.2	0.67
z21	0.72	187.0	1.26	148	7344	0.61970	0.450	23.030	0.46	0.269540	0.061	3109.0	11.0	3228.3	4.4	3303.4	1.0	0.99
z23	0.44	922.0	0.79	1168	60006	0.67977	0.079	27.100	0.11	0.289140	0.046	3343.5	2.1	3387.1	1.1	3413.0	0.8	0.92

Note: Blank composition: $^{206}Pb/^{204}Pb = 18.24 \pm 0.21$; $^{207}Pb/^{204}Pb = 15.34 \pm 0.16$; $^{208}Pb/^{204}Pb = 37.35 \pm 0.20$.

[a]Th contents calculated from radiogenic ^{208}Pb and the $^{207}Pb/^{206}Pb$ date of the sample, assuming concordance between U–Th and Pb systems.

[b]Total mass of radiogenic Pb.

[c]Total mass of common Pb.

[d]Ratio of radiogenic Pb (including ^{208}Pb) to common Pb.

[e]Measured ratio corrected for fractionation and spike contribution only.

[f]Measured ratios corrected for fractionation, tracer, blank, and initial common Pb.

[g]Isotopic dates calculated using the decay constants $\lambda_{238} = 1.55125E-10$ and $\lambda_{235} = 9.8485E-10$ (Jaffey et al. 1971).

Published by NRC Research Press

stants (Mattinson 2000; Schoene et al. 2006). In Fig. 5 and in the text, we report the uncertainties associated with the weighted mean $^{207}Pb/^{206}Pb$ dates as ±*X*/*Y*, where *X* is the internal (analytical) uncertainty and *Y* also includes the decay constant uncertainties (Jaffey et al. 1971). The first reported uncertainty is used when comparing to other $^{207}Pb/^{206}Pb$ dates, and the second when comparing to dates from other isotopic systems (for instance, ^{40}Ar–^{39}Ar). For these $^{207}Pb/^{206}Pb$ dates, tracer calibration does not contribute to uncertainty.

The new U–Pb data in this paper were collected at the Massachusetts Institute of Technology (MIT) Isotope Lab in the mid 1990s and again in 2009–2010. New data from previously dated samples VS 80–13, VS 80–18, HY.z5.81, Drill Arkose, and the Fontano tuff were obtained in 2009–2010. Zircons were separated from crushed samples by standard Wilfley table, magnetic and heavy liquid techniques, then hand picked for clarity and purity under a binocular microscope. Some of the zircons in the older "legacy" (1980s) data were air abraded (Krogh 1982). For the new analyses, zircons were pretreated using a modification of Mattinson's CA–TIMS technique. In the CA method, high-temperature annealing repairs radiation damage in zircon and prevents preferential leaching of Pb relative to U during multistep digestions. Annealed zircons were dissolved in two steps. The initial digestion step preferentially removes radiation-damaged zircon, which is most likely to be affected by postcrystallization Pb loss. This serves to isolate the highest quality low-U zircon for final analysis.

Pretreated grains were spiked with a mixed ^{205}Pb–^{233}U–^{235}U tracer solution and dissolved in HF. Dissolved Pb and U were separated using an HCl-based ion exchange chemistry procedure (modified after Krogh 1973), loaded onto single, degassed Re filaments together with a silica gel-H_3PO_4 emitter, and their isotopic compositions were measured on the VG Sector 54 thermal ionization mass spectrometer (TIMS) at MIT. Isotopic data along with details of fractionation and blank corrections appear in Table 1. The U–Pb data reduction and uncertainty propagation were done with U–Pb_Redux (Bowring et al. 2008; McLean et al. 2008) using the U decay constants of Jaffey et al. (1971). Isotopic data are plotted on standard Concordia plots (Fig. 5).

Results and discussion

Zircons from the felsic tuff near the top of the Vaillant basalt at Vaillant Lake (Fig. 5*f*) are elongate and clear. Seven single abraded grains were analyzed in 1992 and are included in Table 1 but are moderately discordant. In 2009–2010, seven single grains were analyzed using CA–TIMS and six yield a tight cluster of data with a weighted mean $^{207}Pb/^{206}Pb$ date of 2014.32 ± 0.89/6.0, mean square weighted deviation (MSWD) = 0.26 (Fig. 5*a*). We interpret this as the age of its eruption and deposition. This is the first date from the rift sequence beneath Coronation passive margin. The legacy data yield a statistically identical weighted mean $^{207}Pb/^{206}Pb$ date of 2014.65 ± 0.42, MSWD = 1.6, n = 8, demonstrating the relatively simple systematics of these zircons, the fact that CA–TIMS has removed the domains that have lost Pb, and excellent agreement on analyses done 17 years apart.

In the central part of the Slave craton (Fig. 1), a 500 km long by 100 km wide swarm of mafic dykes (Lac de Gras Dykes) trends 010°, parallel to the Coronation margin (LeCheminant 1994; Buchan et al. 2009). The dykes recently yielded $^{207}Pb/^{206}Pb$ baddeleyite dates of 2023 ± 2 and 2027 ± 4, interpreted as ages of dyke emplacement (Buchan et al. 2009). Where the dykes encounter the base of the Paleoproterozoic cover sequence correlative with the Coronation Supergroup, they form differentiated sills (Booth River intrusive suite) with U–Pb zircon ages of 2023 $^{+4}_{-2}$ Ma for the felsic phase (Roscoe et al. 1987), and 2026 ± 1 and 2025 ± 1 Ma for the mafic phase (Davis et al. 2004). These results are 10 million years older on average than the 2014.32 ± 0.89 Ma age reported here for the upper Vaillant felsic tuff. The difference in ages is comparable to the time lags of ~5, ~15, and ~10 million years between flood basalt eruptions and the onset of sea-floor spreading in the North, Central and South Atlantic ocean basins, respectively (Bird et al. 2007; Eagles 2007; Olesen et al. 2007).

Multigrain fractions of zircon from a tongue of the Drill Arkose near Melville Creek (Fig. 3*b*) yielded $^{207}Pb/^{206}Pb$ dates between 2.7 and 3.0 Ga (Bowring 1985), compatible with derivation from Slave craton. For this study, we subjected a large population of zircons to CA–TIMS. Interestingly, after partial dissolution, the inner parts of the grains dissolved leaving an outer shell. Analysis of nine of these partially dissolved grains yield a tight cluster of approximately concordant analyses with a weighted mean $^{207}Pb/^{206}Pb$ date of 2016.45 ± 0.7/0.6, MSWD = 1.1 (Fig. 5*e*). To better understand the results, we subjected an identical population to air abrasion only and analyzed five. Three of these grains give Mesoarchean Pb–Pb dates (ca. 3.3–3.4 Ga), one a date of 2014 Ma like the Vaillant tuff, and two intermediate dates of ca. 2.3–2.4 Ga. We interpret all of these results as indicating syn-rift volcanic zircons (ca. 2014–2016 Ma) with Archean cores, whole Archean grains and geon-23 grains of unknown origin.

The Badlands granite (Fig. 3*b*) was dated by Bowring (1985) and four multigrain discordant analyses yielded an upper intercept of 2589 ± 9 Ma. New data on single grains using CA–TIMS yields a tight cluster of nine analyses with a weighted mean $^{207}Pb/^{206}Pb$ date of 2575.93 ± 0.30/6.6 Ma, MSWD = 1.2 (Fig. 5*b*), which we interpret as the crystallization age of the Badlands granite. This age, combined with those for the Vaillant tuff and Drill arkose, demonstrates that the granite is older than the rift succession and not intrusive into it as previously inferred (Hoffman and Pelletier 1982).

Bowring (1985) analyzed detrital zircons from the Zephyr arkose (sample VS 80–18) of the lower Akaitcho Group (Easton 1980) in the Turmoil klippe at Akaitcho Lake (Fig. 2). He reported isotopic data for eight multigrain fractions made up of uniform populations of euhedral to slightly rounded zircons that defined an upper intercept of 2035 ± 20 Ma. The arkose has distinctive heavy mineral bands rich in zircon and tourmaline. These data were interpreted to reflect derivation from an unknown igneous source of limited age range. Bowring (1985) noted that the largest grains were much more variable and rounded, and chose not to analyze them. In 1993, after it was realized that the Akaitcho Group was not the initial rift sequence of Coronation margin, single

Fig. 5. Analyses of zircons in samples from Wopmay orogen (Fig. 2): (*a*) Igneous zircons from a felsic tuff (sample SAB 91–73) at the top of the Vaillant basalt, Vaillant Lake (Fig. 5*f*); (*b*) Igneous zircons from the Badlands granite (sample HY.z5.81), northwest of Drill Lake (Fig. 3*b*); (*c*) Detrital zircons from the Zephyr arkose (sample VS 80–13), Akaitcho Lake (Fig. 2); (*d*) Igneous zircons in a tuff from the lower Fontano Formation (Recluse Group) in the foreland thrust-fold belt of Wopmay orogen (Fig. 2), previously reported as 1882 ± 4 Ma (Bowring and Grotzinger 1992); (*e*) Detrital zircons from a sandstone tongue (sample HY.z7.81) within the Vaillant basalt, Melville Creek (Fig. 3*b*); (*f*) Collection site (dot) for Vaillant tuff sample SAB91–73 at Vaillant Lake. All uncertainty ellipses are 2σ. The dotted lines are uncertanties in Concordia curve related to decay constants. Weighted mean ^{207}Pb/^{206}Pb dates are shown as insets. Vertical bars are 2σ uncertainties for each zircon, and the light and dark gray fields are 1σ and 2σ uncertainties, respectively, of the weighted mean. Also shown is the weight given each analysis in the weighted mean, presented as box sizes and percentage contributions.

grain analyses for a range of grain sizes from the same rock yielded a more complex picture, with ^{207}Pb/^{206}Pb dates ranging from 1.89 to 2.5 Ga. These analyses, despite vigorous mechanical abrasion, were characterized by discordance related to Pb loss.

For this study, ten of the largest and four of the smallest grains were treated and analyzed by CA–TIMS. Remarkably, the data cluster in two groups on a Concordia diagram, one with a weighted mean ^{207}Pb/^{206}Pb date of 2575.87 ± 0.69/6.6 Ma and the other with a weighted mean date of 1894.70 ± 0.92/5.9 Ma (Fig. 5*c*). This implies that the older population was derived from a point source that is statistically indistinguishable in age from the Badlands granite, 90 km to the north-northeast (Fig. 2). The younger population was likely derived from Akaitcho Group volcanic rocks or plutonic rocks of the Hepburn intrusive suite of Hottah terrane. Either the older age is very well represented in basement rocks of Hottah terrane, or the Zephyr Formation at Akaticho Lake was fed from a small drainage area, consistent with internally drained, active-rift topography. Either way, the identity in age links the Badlands granite to Hottah terrane. In addition, the tourmaline-bearing Badlands granite provides a logical source for detrital tourmaline in the heavy mineral bands of the Zephyr arkose. Consequently, we are forced to conclude that the contact of the granite is faulted, and constitutes a segment of the collisional geosuture between the Turmoil klippe of Hottah terrane (Hildebrand et al. 2010*a*) and the (allochthonous) rifted margin of Slave craton. In fact, allowing for younger conjugate transcurrent faulting, the contact of the Badlands granite is directly on-strike with the leading edge of the Turmoil klippe to the south (Figs. 2 and 3*a*; Hildebrand et al. 2010*a*; Hildebrand 2011).

Bowring and Grotzinger (1992) published an age for the drowning of the passive margin during its collision with the Hottah Terrane, based on a concordia upper intercept date of 1882 ± 4 Ma for a tuff near the base of the foredeep succession west of Eokuk Lake (Fig. 2). Six new analyses of zircons from this sample confirm the date and refine it to 1882.50 ± 0.95/5.9 Ma (Fig. 5*d*). If 2014.32 ± 0.89 Ma is the age of the rift-to-drift transition and 1882.50 ± 0.95 Ma is the age of the passive margin's destruction, then the duration of the passive margin was ~132 million years. This is close to the mean duration of 137 million years (n = 15) for Cambrian–Carboniferous passive margins and 130 million years (n = 13) for extinct Permian–Neogene examples (Bradley 2008).

Conclusions

A U–Pb zircon date of 2014.32 ± 0.89 Ma was obtained from a felsic tuff at the top of a rift-related basalt pile (Vaillant basalt) at the allochthonous western paleomargin of Slave craton in Wopmay orogen. The date is ~10 million years younger than a major swarm of diabase dykes (Lac de Gras dykes) and related differentiated sills (Booth River intrusive suite) in the central part of the craton. A tongue of clastic sedimentary rocks (Drill arkose) within the Vaillant basalt has mixed 2016.45 ± 0.70 Ma (synvolcanic) and Mesoarchean (3.3–3.4 Ga) detrital zircon dates, the latter compatible with derivation from Slave craton. In contrast, detrital zircon dates from the Zephyr arkose (lower Akaticho Group) within the Turmoil klippe of Hottah terrane contain a mixed population with ^{207}Pb/^{206}Pb dates that range from 2.59 to 1.88 Ga. A subset of the largest grains cluster tightly at 2575.87 ± 0.39 Ma, a date that is statistically indistinguishable from the crystallization age of 2575.93 ± 0.30 Ma obtained from the Badlands granite. Assuming the Zephyr arkose of Hottah terrane was derived in part from the Badlands granite or equivalent body, the tectonic contact between the Badlands granite and the Drill–Vaillant rift assemblage must represent a segment of the geosuture between Hottah terrane and the Coronation margin of Slave craton. The 2014.32 ± 0.89 Ma age for the rift-to-drift transition and the 1882.50 ± 0.95 Ma age for the arrival of the passive margin at the Calderian subduction zone suggest a duration of ~132 million years for the passive margin. This is similar to the mean age of extinct Phanerozoic passive margins of ~134 million years (Bradley 2008).

Acknowledgments

Field work by P.F. Hoffman and R.S. Hildebrand in Wopmay orogen contributed to mapping projects of the former Precambrian Subdivision under J.C. McGlynn, Geological Survey of Canada. R.M. Easton, J.P. Grotzinger, K.S. Pelletier, M.R. St-Onge, and R. Tirrul also contributed to the mapping. Mapping and sample collection in Wopmay orogen by SAB was generously supported from 1980–1985 by W.A. Padgham in the Yellowknife office of the Department of Indian and Northern Affairs. Laboratory work was supported by W.R. Van Schmus at the University of Kansas from 1979–1983 with funding from the U.S. National Science Foundation. Bowring's 1992 expedition to find dateable material in the Vaillant basalt with the late Todd Housh was made possible with helicopter time provided by W.A. Padgham. We thank Ken Buchan, Tony LeCheminant,

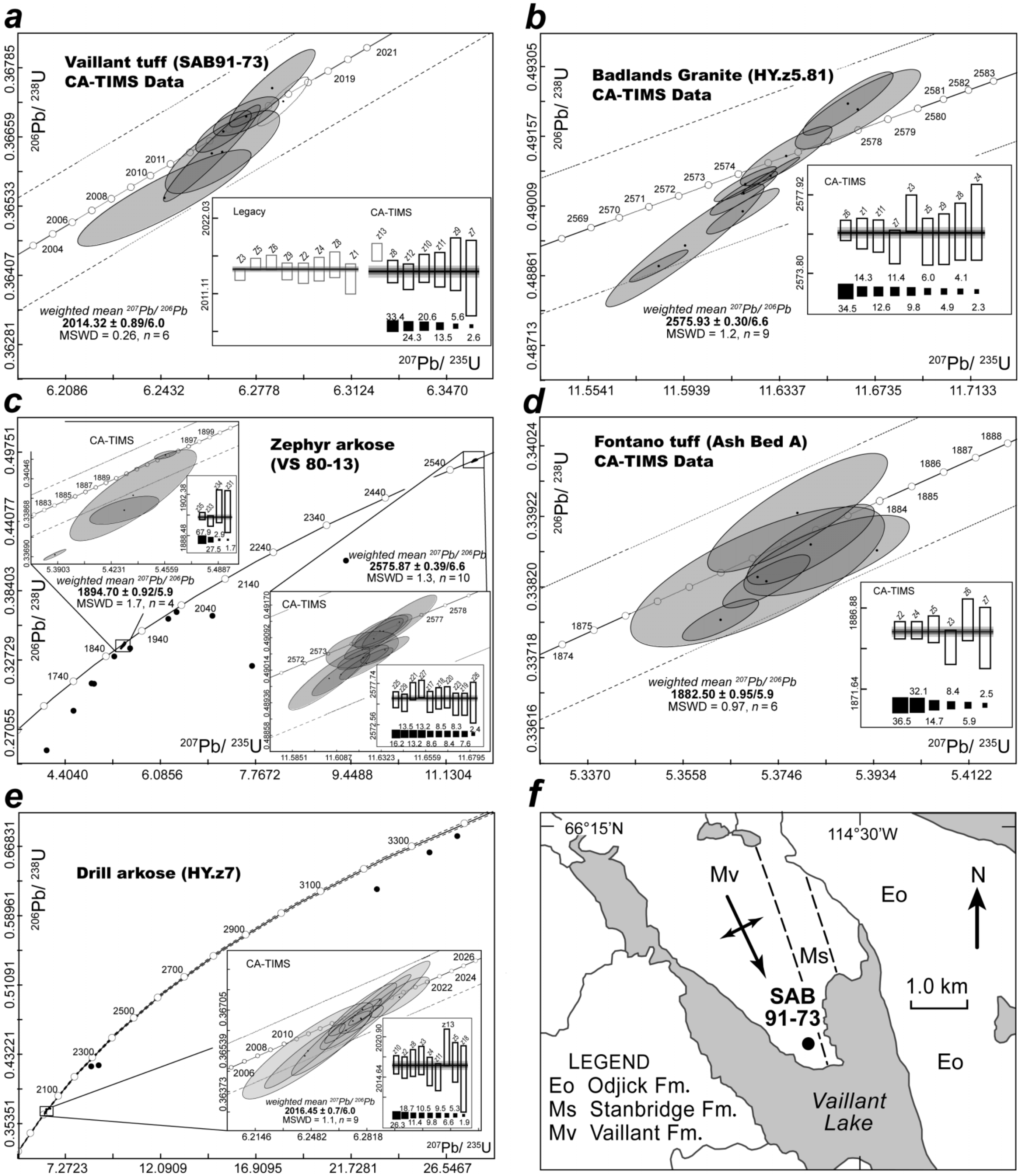
a
Vaillant tuff (SAB91-73)
CA-TIMS Data
Legacy
CA-TIMS
weighted mean 207Pb/206Pb
2014.32 ± 0.89/6.0
MSWD = 0.26, n = 6
b
Badlands Granite (HY.z5.81)
CA-TIMS Data
weighted mean 207Pb/206Pb
2575.93 ± 0.30/6.6
MSWD = 1.2, n = 9
c
Zephyr arkose
(VS 80-13)
weighted mean 207Pb/206Pb
1894.70 ± 0.92/5.9
MSWD = 1.7, n = 4
weighted mean 207Pb/206Pb
2575.87 ± 0.39/6.6
MSWD = 1.3, n = 10
d
Fontano tuff (Ash Bed A)
CA-TIMS Data
weighted mean 207Pb/206Pb
1882.50 ± 0.95/5.9
MSWD = 0.97, n = 6
e
Drill arkose (HY.z7)
weighted mean 207Pb/206Pb
2016.45 ± 0.7/6.0
MSWD = 1.1, n = 9
f
66°15'N
114°30'W
Mv
Ms
Eo
N
1.0 km
SAB
91-73
LEGEND
Eo Odjick Fm.
Ms Stanbridge Fm.
Mv Vaillant Fm.
Vaillant
Lake

and Otto van Breemen for a preprint of their paper on the Lac de Gras dyke swarm. The paper was substantially improved thanks to careful reviews by W. Bleeker, W. Davis, and an anonymous referee.

References

Bird, D.E., Hall, S.A., Burke, K., Casey, J.F., and Sawyer, D.S. 2007. Early Central Atlantic Ocean seafloor spreading history. Geosphere, **3**(5): 282–298. doi:10.1130/GES00047.1.

Bowring, S.A. 1985. U–Pb zircon geochronology of early Proterozoic Wopmay orogen, N.W.T., Canada: an example of rapid crustal evolution. Ph.D. thesis, University of Kansas, Lawrence, Kansas, 148 p.

Bowring, S.A., and Grotzinger, J.P. 1992. Implications of new chronostratigraphy for tectonic evolution of Wopmay orogen, northwest Canadian Shield. American Journal of Science, **292**: 1–20.

Bowring, S.A., and Podosek, R.A. 1989. Nd isotopic evidence from Wopmay orogen for 2.0–2.4 Ga crust in western North America. Earth and Planetary Science Letters, **94**(3–4): 217–230. doi:10.1016/0012-821X(89)90141-6.

Bowring, J.F., McLean, N.M., Walker, J.D., and Bowring, S.A. 2008. Building cyberinfrastructure for geochronology: software engineering meets geochemistry. Geological Society of America Abstracts with Programs, **40**(6): 136.

Bradley, D.C. 2008. Passive margins through earth history. Earth-Science Reviews, **91**(1-4): 1–26. doi:10.1016/j.earscirev.2008.08.001.

Buchan, K.L., LeCheminant, A.N., and van Breemen, O. 2009. Paleomagnetism and U–Pb geochronology of the Lac de Gras diabase dyke swarm, Slave Province, Canada: implications for relative drift of Slave and Superior provinces in the Paleoproterozoic. Canadian Journal of Earth Sciences, **46**(5): 361–379. doi:10.1139/E09-026.

Cawood, P.A., McCausland, P.J.A., and Dunning, G.R. 2001. Opening Iapetus: constraints from the Laurentian margin of Newfoundland. Geological Society of America Bulletin, **113**(4): 443–453. doi:10.1130/0016-7606(2001)113<0443:OICFTL>2.0.CO;2.

Cook, F.A., van der Velden, A.J., Hall, K.W., and Roberts, B.J. 1999. Frozen subduction in Canada's Northwest Territories: Lithoprobe deep lithospheric reflection profiling of the western Canadian Shield. Tectonics, **18**(1): 1–24. doi:10.1029/1998TC900016.

Davis, R.E., and Bleeker, W. 2007. New ages for Paleoproterozoic mafic intrusions in the western Slave Province and their potential relationship to tectonic events in the adjacent Wopmay orogen. Geological Association of Canada, Abstracts with Programs, **32**: 20.

Davis, R.E., Bleeker, W., Hulbert, L., and Jackson, V. 2004. New geochronological results from the Slave Metallogeny Project. *In* 32nd Annual Yellowknife Geoscience Forum Abstracts, 29004. pp. 20.

Eagles, G. 2007. New angles on South Atlantic opening. Geophysical Journal International, **168**(1): 353–361. doi:10.1111/j.1365-246X.2006.03206.x.

Easton, R.M. 1980. Stratigraphy and geochemistry of the Akaitcho Group, Hepburn Lake map area, District of Mackenzie: an initial rift succession in Wopmay orogen (Early Proterozoic). *In* Current Research, Part B. Geological Survey of Canada, Paper 80-1B, pp. 47–57.

Easton, R.M. 1981. Stratigraphy of the Akaitcho Group and development of an early Proterozoic continental margin, Wopmay orogen, Northwest Territories. *In* Proterozoic basins in Canada. *Edited by* F.H.A. Campbell. Geological Survey of Canada, Paper 81-10, pp. 79–95.

Easton, R.M. 1983. Crustal structure of rifted continental margins: geological constraints from the Proterozoic rocks of the Canadian shield. Tectonophysics, **94**(1–4): 371–390. doi:10.1016/0040-1951(83)90025-2.

Fraser, J.A., Hoffman, P.F., Irvine, T.N., and Mursky, G. 1971. The Bear Province. *In* Variations in Tectonic Styles in Canada. *Edited by* R.A. Price, and R.J.W. Douglas. Geological Association of Canada, Special Publication 11, pp. 453–504.

Grotzinger, J.P. 1986. Evolution of Early Proterozoic passive-margin carbonate platform, Rocknest Formation, Wopmay orogen, Northwest Territories, Canada. Journal of Sedimentary Research, **56**: 831–847.

Hibbard, J.P., van Staal, C.R., Rankin, D.W., and Williams, H. 2005. Geology, lithotectonic map of the Appalachian orogen. Geological Survey of Canada, Map 02041A, scale 1 : 1 500 000.

Hildebrand, R.S. 2011. Geological synthesis of northern Wopmay orogen and Coppermine homocline, Northwest Territories – Nunavut. Geological Survey of Canada, Open File 6390 (geological map, scale 1 : 500 000).

Hildebrand, R.S., Hoffman, P.F., and Bowring, S.A. 1987. Tectonomagmatic evolution of the 1.9 Ga Great Bear magmatic zone, Wopmay orogen, northwestern Canada. Journal of Volcanology and Geothermal Research, **32**(1–3): 99–118. doi:10.1016/0377-0273(87)90039-4.

Hildebrand, R.S., Bowring, S.A., and Housh, T. 1990. The medial zone of Wopmay orogen, District of Mackenzie. Current Research, Part C. Geological Survey of Canada, Paper 90-1C, pp. 167–176.

Hildebrand, R.S., Paul, D., Pietkainen, P., Hoffman, P.F., Bowring, S.A., and Housh, T. 1991. New geological developments in the internal zone of Wopmay orogen, District of Mackenzie. *In* Current Research, Part C. Geological Survey of Canada, Paper 91-1C, pp. 157–164.

Hildebrand, R.S., Hoffman, P.F., and Bowring, S.A. 2010*a*. The Calderian orogeny in Wopmay Orogen (1.9 Ga), northwestern Canadian Shield. Geological Society of America Bulletin, **122**(5–6): 794–814. doi:10.1130/B26521.1.

Hildebrand, R.S., Hoffman, P.F., Housh, T., and Bowring, S.A. 2010*b*. The nature of volcano–plutonic relations and the shapes of epizonal plutons of continental arcs as revealed in the Great Bear magmatic zone, northwestern Canada. Geosphere, **6**: 1–28. doi:10.1130/GES00533.1.

Hoffman, P.F. 1973. Evolution of an early Proterozoic continental margin: the Coronation geosyncline and associated aulacogens, northwest Canadian shield. *In* Evolution of the Precambrian crust. *Edited by* J. Sutton and J.F. Windley. Philosphical Transactions of the Royal Society, London. Series A, 273: 547–581.

Hoffman, P.F. 1980. Wopmay orogen: a Wilson cycle of Early Proterozoic age in the northwest of the Canadian shield. *In* Continental crust and its mineral deposits. *Edited by* D.W. Strangway. Geological Association of Canada, Special Publication 20, pp. 523–549.

Hoffman, P.F. 1987*a*. Continental transform tectonics, Great Slave Lake shear zone (ca 1.9 Ga), northwest Canada. Geology, **15**(9): 785–788. doi:10.1130/0091-7613(1987)15<785:CTTGSL>2.0.CO;2.

Hoffman, P.F. 1987*b*. Proterozoic foredeeps, foredeep magmatism, and Superior-type iron-formation in the Canadian shield. *In* Proterozoic lithospheric evolution. *Edited by* A. Kröner. American Geophysical Union, Geodynamics Series 17, pp. 85–97.

Hoffman, P.F., and Bowring, S.A. 1984. Short-lived 1.9 Ga continental margin and its destruction, Wopmay orogen, northwest

Canada. Geology, **12**(2): 68–72. doi:10.1130/0091-7613(1984)12<68:SGCMAI>2.0.CO;2.

Hoffman, P.F., and Hall, L. 1993. Geology, Slave craton and environs. Geological Survey of Canada, Open File 2559 (geological map, scale 1 : 1 000 000).

Hoffman, P.F., and McGlynn, J.C. 1977. Great Bear batholith: A volcano-plutonic depression. *In* Volcanic Regimes in Canada. *Edited by* W.R.A. Baragar, L.C. Coleman, and J.M. Hall. Geological Association of Canada, Special Publication 16, pp. 169–192.

Hoffman, P.F., and Pelletier, K.S. 1982. Cloos nappe in Wopmay orogen: significance for stratigraphy and structure of the Akaitcho Group, and implications for opening and closing of an early Proterozoic continental margin. *In* Current research, Part A. Geological Survey of Canada, Paper 82-1A, pp. 109–115.

Hoffman, P.F., and Tirrul, R. 1994. Geology, northern externides of Wopmay orogen, District of Mackenzie. Geological Survey of Canada, Open File 3251 (geological map, scale 1 : 250 000).

Hoffman, P.F., Fraser, J.A., and McGlynn, J.C. 1970. The Coronation geosyncline of Aphebian age, northwestern Canadian shield. *In* Precambrian Basins and Geosynclines of the Canadian Shield. *Edited by* A.J. Baer. Geological Survey of Canada, Paper 70-40, pp. 200–212.

Hoffman, P.F., St-Onge, M.R., Carmichael, D.M., and de Bie, I. 1978. Geology of the Coronation Geosyncline (Aphebian), Hepburn Lake area, District of Mackenzie. *In* Current research, Part A. Geological Survey of Canada, Paper 78-1A, pp. 147–151.

Hoffman, P.F., St-Onge, M.R., Easton, R.M., Grotzinger, J., and Schulze, D.E. 1980. Syntectonic plutonism in north-central Wopmay orogen (Early Proterozoic), Hepburn Lake map area, District of Mackenzie. *In* Current research, Part A. Geological Survey of Canada Paper, 80-1A, pp. 171–177.

Housh, T., Bowring, S.A., and Villeneuve, M. 1989. Lead isotopic study of early Proterozoic Wopmay orogen, NW Canada: Role of continental crust in arc magmatism. The Journal of Geology, **97**(6): 735–747. doi:10.1086/629355.

Irving, E., Baker, J., Hamilton, M., and Wynne, P.J. 2004. Early Proterozoic geomagnetic field in western Laurentia: implications for paleolatitudes, local rotations and stratigraphy. Precambrian Research, **129**(3–4): 251–270. doi:10.1016/j.precamres.2003.10.002.

Jaffey, H., Flynn, K.F., Glendenin, L.E., Bentley, W.C., and Essling, A.M. 1971. Precision measurement of half-lives and specific activities of ^{235}U and ^{238}U. Physical Review, **4**: 1889–1906.

Krogh, T.E. 1973. A low-contamination method for hydrothermal decomposition of zircon and extraction of U and Pb for isotopic age determinations. Geochimica et Cosmochimica Acta, **37**: 485–494.

Krogh, T.E. 1982. Improved accuracy of U–Pb zircon ages by creation of more concordant systems using an air abrasion technique. Geochimica et Cosmochimica Acta, **46**(4): 637–649. doi:10.1016/0016-7037(82)90165-X.

Krogh, T.E., and Davis, G.L. 1971. Zircon U–Pb ages of Archaean metavolcanic rocks in the Canadian Shield. Carnegie Institution of Washington. Geophysical Laboratory Report for 1970–71, pp. 241–242.

Kuenen, P.H. 1950. The formation of the continental terrace. Advancement of Science, **7**: 76–80.

LeCheminant, A.N. 1994. Proterozoic diabase dyke swarms; Lac de Gras and Aylmer Lake area, District of Mackenzie, Northwest Territories. Geological Survey of Canada, Open File 2975 (geological map, scale 1 : 250 000).

Mattinson, J.M. 1987. U–Pb ages of zircons: a basic examination of error propagation. Chemical Geology (Isotope Geoscience Section), **66**: 151–162.

Mattinson, J.M. 2000. Revising the "gold standard": the Uranium decay constants of Jaffe et al., 1971. EOS, Transactions of the American Geophysical Union 2000 Spring Meeting, Vol. 81(19), 9 May 2000, Supplement.

Mattinson, J.M. 2005. Zircon U–Pb chemical abrasion (CA–TIMS) method: Combined annealing and multi-step partial dissolution analysis for improved precision and accuracy of zircon ages. Chemical Geology, **220**(1–2): 47–66. doi:10.1016/j.chemgeo.2005.03.011.

McLean, N.M., Bowring, J.F., Bowring, S.A., and Schoene, R.B. 2008. More than just an age: quantitative analysis of geochronological data and uncertainty. Geological Society of America Abstracts with Programs, **40**(6): 134.

Nance, R.D., and Linnemann, U. 2008. The Rheic Ocean: origin, evolution, and significance. GSA Today, **18**(12): 4–12. doi:10.1130/GSATG24A.1.

Olesen, O., Ebbing, J., Lundin, E., Mauring, E., Skilbrei, J.R., Torsvik, T.H., et al. 2007. An improved tectonic model for the Eocene opening of the Norwegian–Greenland Sea: Use of modern magnetic data. Marine and Petroleum Geology, **24**(1): 53–66. doi:10.1016/j.marpetgeo.2006.10.008.

Roscoe, S.M., Henderson, M.N., Hunt, P.A., and van Breemen, O. 1987. U–Pb zircon age of an alkaline granite body in the Booth River Intrusive Suite, N.W.T. *In* Radiogenic age and isotopic studies: Report 1. Geological Survey of Canada, Paper 87-2, pp. 95–100.

Schoene, B., Crowley, J.L., Condon, D.C., Schmitz, M.D., and Bowring, S.A. 2006. Reassessing the uranium decay constants for geochronology using ID–TIMS data. Geochimica et Cosmochimica Acta, **70**: 426–445.

Sprigg, R.C. 1952. Sedimentation in the Adelaide Geosyncline and the formation of the continental terrace. *In* Sir Douglas Mawson Anniversary Volume. *Edited by* M.F. Glaessner and E.S. Rudd. The University of Adelaide, Adelaide, South Australia, pp. 153–159.

van Staal, C.R., Dewey, J.F., Mac Niocaill, C., and McKerrow, W.S. 1998. The Cambrian-Silurian tectonic evolution of the northern Appalachians and British Caldeonides: history of a complex, west and southwest Pacific-type segment of Iapetus. *In* Lyell: the past is the key to the present. *Edited by* D.J. Blundell and A.C. Scott. Geological Society of London, Special Publication 143, pp. 199–242.

van Staal, C.R., Whalen, J.B., Valverde-Vaquero, P., Zagorevski, A., and Rogers, N. 2009, Pre-Carboniferous, episodic accretion-related, orogenesis along the Laurentian margin of the northern Appalachians. *In* Ancient orogens and modern analogues. *Edited by* J.B. Murphy, J.D. Keppie, and A.J. Hynes. Geological Society of London, Special Publication 327, pp. 271–316.

Villeneuve, M.E. 1988. Pb isotopes as evidence for an early Proterozoic source for garnet granites of Wopmay orogen, N.W.T. M.A. thesis, University of Kansas, Lawrence, Kansas, 136 p.